2019

Proteomic analysis for phenanthrene-elicited wheat chloroplast deformation

Yu Shen
Nanjing Agricultural University

Jinfeng Li
Nanjing Agricultural University

Ruochen Gu
Nanjing Agricultural University

Xinhua Zhan
Nanjing Agricultural University

Baoshan Xing
University of Massachusetts Amherst, bx@umass.edu

Shen, Yu; Li, Jinfeng; Gu, Ruochen; Zhan, Xinhua; and Xing, Baoshan, "Proteomic analysis for phenanthrene-elicited wheat chloroplast deformation" (2019). *Environmental International*. 4.
https://doi.org/10.1016/j.envint.2018.11.074

Environment International 123 (2019) 273–281

Contents lists available at ScienceDirect

Environment International

journal homepage: www.elsevier.com/locate/envint

Proteomic analysis for phenanthrene-elicited wheat chloroplast deformation

Yu Shen[a,b], Jinfeng Li[a], Ruochen Gu[a], Xinhua Zhan[a,*], Baoshan Xing[b]

[a] College of Resources and Environmental Sciences, Nanjing Agricultural University, Nanjing, Jiangsu Province 210095, China
[b] Stockbridge School of Agriculture, University of Massachusetts, Amherst, MA 01003, USA

ARTICLE INFO

Handling editor: Yong-Guan Zhu

Keywords:
Polycyclic aromatic hydrocarbons
Leaf cell
Proteomics
Chloroplast deformation
Toxicity
iTRAQ

ABSTRACT

The exposure of polycyclic aromatic hydrocarbons (PAHs) can cause wheat leaf chlorosis. Thus, we hypothesize that chloroplast inner structure damage is the reason for leaf chlorosis. This study was conducted with the wheat seedlings exposed to Hoagland nutrient solution containing 1.0 mg L^{-1} phenanthrene for 9 days. Subcellular observation showed that chloroplast turns round and loses its structural integrity. Herein, iTRAQ (isobaric tag for relative and absolute quantification) was applied to analyze the changes of protein profile in chloroplast exposed to phenanthrene. A total of 517 proteins are identified, 261 of which are up-regulated. Eight proteins related with thylakoid (the structural component of chloroplast) are down-regulated and the expression of related genes further confirms the proteomic results through real-time PCR under phenanthrene treatment, suggesting that the thylakoid destruction is the reason for chloroplast deformation. Four proteins related with envelope and stroma are up-regulated, and this is the reason why chloroplast remains round. This study is useful in discussing the carcinogenic and teratogenic effects of PAHs in plant cells in the environment, and provides necessary knowledge for improving crop resistance to PAH pollution.

1. Introduction

Polycyclic aromatic hydrocarbons (PAHs) are a group of over 100 toxic organic compounds with two or more fused benzene rings. They are hydrophobic and recalcitrant in the environment, and carcinogenic, teratogenic and mutagenic to humans and animals (Ali et al., 2017; Davie-Martin et al., 2017). Most of the environmental PAHs exist in surface soil and dissipate slowly (Jia et al., 2017). Surface soil is essential for plant growth and agricultural activities (Bordajandi et al., 2004). Therefore, PAHs pose a threat to crop security. In the legislations of US EPA, European Union and China, the limited PAH concentrations in water or food are lower than 0.2 μg L^{-1}, 30 μg kg^{-1} and 10 μg kg^{-1}, respectively (Zelinkova and Wenzl, 2015). There are many reports about the negative growth effects caused by the accumulation of PAHs in crops. Under the stress of phenanthrene and pyrene, > 25 % biomass and over 37 % chlorophyll *b* concentraion would decrease in *Oryza sativa* (Li et al., 2008). In the phenanthrene treatment, wheat seed germination rates were reduced over 32 %, and photosystem function of the seedlings decreased by 20 % (Wei et al., 2008). Since chloroplast is the unique organelle for plants to receive and transfer light energy in biosphere (Sharkey, 2005), the understanding of chloroplast response to PAH pollution would be important to understand the mechanism underlying PAH working against its structure and function change and to improve the cognition of safe cropping systems and phytoremediation for the PAH-contaminated environment.

It is well-known that photosynthesis is the ultimate source of energy for all the activities in plant life (Käpylä et al., 2009; de Lucia et al., 2014). In previous study, we found that the accumulation of phenanthrene triggers wheat leaf chlorosis from its base (Shen et al., 2017). Chloroplast is the only pigment carrier in higher plants, and its safety is a concern on the crop yield (Ron and Walter, 2007). The change in protein structure and quantity can affect the activity of organelle and cell under stress (Andersson and Anderson, 1980). Accordingly, the analysis of chloroplast protein change would be a new aspect to understand energy metabolism and matter cycle in plants under PAH treatments. However, there is no report on the changes of chloroplast structure and function upon expousre to PAHs. Proteins serve a variety of functions within cells, such as structural support, movement of cell, enzymatic activity, and genetic expression (Aebersold and Mann, 2016). In the PAH contaminated soil, three proteins with clonal differences were identified through proteomics in birch, and ferritin-like protein, auxin-induced protein and peroxidase were differentially expressed under anthracene, fluoranthene, phenanthrene and pyrene treatments (Tervahauta et al., 2009). With the stress of benzo(a)pyrene in *Thalassiosira pseudonana*, about 10 % of the identified proteins were regulated, and the silicon transporter and its gene expression were

* Corresponding author.
E-mail address: xhzhan@njau.edu.cn (X. Zhan).

https://doi.org/10.1016/j.envint.2018.11.074
Received 8 October 2018; Received in revised form 22 November 2018; Accepted 29 November 2018
Available online 12 December 2018

confirmed as the regulation effect in plants (Carvalho and Lettieri, 2011). Under phenanthrene treatment, five proteins related to plant defense response, antioxidant system and glycolysis are up-regulated, and three proteins related to metabolism of high-energy compounds and plant growth become down-regulated in root plasma membrane through proteomic analysis (Shen et al., 2016). Nonetheless, there is no detailed information about chloroplast protein response under abiotic stress.

Proteomics is the large-scale study of proteins (Anderson and Anderson, 1998). In recent years, proteomics is an important complement to investigations at the genomic, transcriptomic and metabolomic level (Agrafiotis et al., 2002; Bensmail and Haoudi, 2003), because proteins execute and control most biochemical processes in organic cells (Hood and Rowen, 2013; Anderson et al., 2016). Under heavy metal pollution, Mustafa and Komatsu (2016) concluded the heavy metal toxicity mechanism by proteomic analysis in plants, and confirmed that glutathione cycle helps cell regulation in metal detoxification. Proteomics has also been applied to detect the mechanisms of drought tolerance in rice, and the expressions of small GTPase and V-ATPase proteins were the key points (Mirzaei et al., 2012). Also a great number of important housekeeping proteins were released in *Chlamydomonas reinhardtii*, and the proteomics offers the useful information about plant tolerance protein response to salinity stress (Yokthongwattana et al., 2012). As yet, proteomics has been applied to analyze the structural and functional changes in biology, and becomes a hot spot in environmental PAH stress research (Carvalho and Lettieri, 2011; El Amrani et al., 2015). With the development of proteomics, isobaric tag for relative and absolute quantitation (iTRAQ) has been widely used in environmental biology (Lan et al., 2010), and iTRAQ is a technology that utilizes isobaric reagents to label the primary amines of peptides and proteins and is used in proteomics to study quantitative changes in the proteome by tandem mass spectrometry (Muth et al., 2010). Generally, iTRAQ-based quantitation facilitates the comparative analysis of peptides and proteins in a variety of settings including comparisons of normal or treated states (Vélez-Bermúdez et al., 2016). This method has been also applied in organelle proteomics (Gonczarowska-Jorge et al., 2017; Lande et al., 2017). Recently, the proteomic reports are more at plant tissue level through 2-dimensional gel electrophoresis (2-DE) proteomics rather than organelle proteomics. To gain a better understanding of structural and functional protein responses under PAH treatment, we applied iTRAQ label analysis here. As we know, it is the first report about the chloroplast proteomics under exposure to PAHs.

In this study, it is hypothesized that PAH exposure would induce chloroplast functional protein decline, and then lead to chloroplast structural damage in wheat leaf. The aims of this study were (1) to characterize the chloroplast structure change under PAH treatment and reveal the molecular mechanism on chloroplast deformation, and (2) to offer new evidence for the carcinogenicity and teratogenicity caused by PAHs in plants.

2. Materials and methods

2.1. Plant preparation and phenanthrene treatment

Wheat (*Triticum aestivum* L. cv. NAU 9918) seeds were surface-sterilized with 3% H_2O_2 for 5 min, and then germinated on moistened filter paper for 4 days at 25 °C in the dark after being thoroughly rinsed with Millipore water (Milli-Q, Billerica, MA, USA). The wheat seedlings were transplanted to black plastic pot containing 2500 mL half-strength aerated Hoagland nutrient solution for 5 days and then transferred to the full-strength Hoagland solution for another 5 days under controlled conditions (photoperiod 16 h light/8 h dark, light intensity of 400 μmol $m^{-2} s^{-1}$, day/night temperature of 25/20 °C, relative humidity of 60%). The nutrient solution prepared with Millipore water, and the initial pH of the solution was adjusted to 5.5.

After a 10-day growth in Hoagland nutrient solution, the wheat seedlings were immersed in Millipore water for 24 h and then divided into two groups: Hoagland nutrient solution (pH 5.5) without phenanthrene (control) and Hoagland nutrient solution (pH 5.5) with 1.0 mg L^{-1} phenanthrene. The phenanthrene-treating time was 9 days. During the exposure time, we replenished the solution every two days with the same treated solution, and added the solution to the volume when the exposure experiment began. There were quadruplicates in each treatment. Phenanthrene, a model PAH, was purchased from Fluka Chemical Corporation (phenanthrene purity > 97%). Its molecular weight is 178.2 g mol^{-1}, and its water solubility is 1.3 mg L^{-1} at 25 °C.

2.2. Chloroplast ultrastructure observation

Transmission electron microscopy (TEM) was applied to observe the chloroplast ultrastructure changes in wheat leaf under control and two phenanthrene treatments (0.5 and 1.0 mg L^{-1}) after 10 days. Wheat leaves were cut into 1 mm^2 segments and placed immediately in freshly prepared mixture of 3% (w/v) glutaraldehyde in 0.05 M phosphate buffer (pH 7.2) for 24 h at 4 °C and post-fixed in 2% aqueous osmium tetroxide in the same buffer for 2 h. After post-fixation, the samples were dehydrated in a gradient series of acetone/alcohol, infiltrated and embedded in London Resin (LR). Ultra-thick sections (50–70 nm) were made with a glass knife on a Leica ultra-cut (UCT-GA-D/E-1/00) microtome. Ultra-thick sections were mounted on Cu grids and stained with saturated aqueous uranyl acetate and post-stained with 4% citrate. At last, the ultrastructure of the sections was observed by TEM (Hitachi, H-3000 N) (Bozzola, 2007).

2.3. Chloroplast extraction

The extraction method (Percoll gradient centrifugation) was based on the method by Grabsztunowicz and Jackowski (2012) with some modifications. For chloroplast protein preparation, 10 g of wheat leaf samples of control or phenanthrene treatment were homogenized in 25 mL of ice-cold (0 to 2 °C) isolation buffer containing 2 mM EDTA, 50 mM 4-(2-hydroxyethyl)-1-piperazineethanesulfonic acid (HEPES)/NaOH (pH 8.0), 1 mM NaCl, 1 mM $MgCl_2$, 0.33 mM sorbitol, 5 mM ascorbic acid and freshly added 0.2% bovine serum albumin (BSA) by using a motor-driven blender (50 Hz). After filtration of the homogenate through a 100 μm filter (BD Falcon, USA), the cleared homogenate was centrifuged at 29,000*g* for 15 min at 4 °C. The filtrate was centrifuged for 5 min at 2600*g* to sediment chloroplasts into a green pellet, which was then resuspended in the ice-cold isolation buffer. The chloroplast suspension was then loaded on the top of linear Percoll gradient solution (2 mM EDTA, 50 mM HEPES/NaOH (pH 8.0), 1 mM NaCl, 1 mM $MgCl_2$, 0.33 mM sorbitol, 50% Percoll, 3% polyethylene glycol 6000 (PEG 6000), 1% BSA and 1% Ficoll), then precentrifuged at 43,000*g* for 30 min at 4 °C, and centrifuged in a swing-out rotor for 10 min at 10,500*g* at 4 °C (brake off). Intact chloroplasts were collected from the gradients (lower band), diluted three times in isolation buffer without BSA and centrifuged at 3300*g* for 5 min at 4 °C. The supernatant was discarded and the washed chloroplast pellet was collected.

2.4. Digestion and iTRAQ labeling

The extracted chloroplast samples (500 μg each) were dissolved with 10 mM dithiothreitol (DTT), alkylated with 55 mM iodoacetamide and digested with sequencing-grade trypsin (V5111, Promega, CA, USA) using the filtered aide sample preparation (FASP) method (Wiśniewski et al., 2009). After trypsin digestion, about 60 μg peptides of each sample were labeled separately using the iTRAQ 8-plex kits (Sigma-Aldrich, USA) (113, 114, 115 and 116 for the phenanthrene-treated chloroplast proteins, 117, 118, 119 and 121 for the control ones) according to the manufacturer's protocol. After being labeled and quenched, the samples were combined and dried by vacuum

centrifugation.

2.5. MS/MS analysis using an LTQ-Orbitrap XL

Each sample was reconstituted in buffer A (2% acetonitrile (ACN) and 0.1% formic acid (FA)) and centrifuged at 20, 000 *g* for 10 min. Using an auto sampler, 20 μL of supernatant were loaded onto a 2 cm C_{18} trap column (inner diameter 200 μm) on a nano HPLC (Thermo Fisher Scientific, USA). The peptides were eluted onto a resolving 10 cm analytical C_{18} column (inner diameter 75 μm) that was assembled in-house. The samples were loaded at 4 μL min^{-1} for 8 min and eluted with an 88 min gradient at 400 nL min^{-1} from 3 to 28% buffer B (98% ACN, 0.1% FA), 20 min from 28 to 55% buffer B, followed by a 5 min linear gradient to 98% buffer B, maintenance at 98% buffer B for 20 min, and finally a return to 3% buffer B over 1 min. The peptides were subjected to nano electrospray ionization followed by tandem mass spectrometry (MS/MS) in an LTQ-Orb iTRAQ XL (Thermo Fisher Scientific, CA, USA) coupled online to the HPLC. Intact peptides were detected in the Orbitrap with a resolution of 60, 000 (all Orbitrap system resolution values are given at *m/z* 400). Peptides were selected for MS/MS using the high-energy collision dissociation (HCD) operating mode with a normalized collision energy setting of 40.0%; ion fragments were detected in the orbitrap at a resolution of 7500. A data-dependent procedure that alternated between one MS scan followed by 5 MS/MS scans was applied for the 5 most abundant precursor ions above a threshold ion for 5000 counts in the MS survey scan, with a duration of 60 s. The electrospray voltage applied was 2.4 kV. Automatic gain control (AGC) was used to optimize the spectra generated by the orbitrap. The AGC target for the full MS was 1e6 and 1e5 for MS2. For the MS scans, the m/z scan range was 350–1800 Da. For the MS2 scans, the m/z scan range was 100–1800.

2.6. Database search and iTRAQ quantification

The samples were analyzed by nano-LC-MS/MS (Thermo Fisher Scientific, USA). The peak lists were generated with Proteome Discoverer 1.3 (Thermo Fisher Scientific, CA, USA). The proteins were identified using the SEQUEST search engine by searching against the NCBI database (October 27th, 2016). For protein identification, a mass tolerance of 10 peptide mass fingerprinting (PMF) was permitted for the intact peptide masses and 0.02 Da for the fragmented ions, with an allowance for one missed cleavage in the trypsin digests. Oxidation at methionine was set as the potential variable modifications, whereas carbamidomethylation at cysteine was set as the fixed modification. The charge states of the peptides were set to +2 and +3. Specifically, an automatic decoy database search was performed in SEQUEST by choosing the decoy checkbox in which a random sequence of the database is generated and tested for the raw spectra, as well as the real database. Only peptides identified at the 99% confidence interval by a SEQUEST probability analysis were counted and each identified protein included at least one unique peptide to reduce the probability of false identification. Only proteins that were identified in all four independent tests were considered. In this study, a protein with a fold change of > 1.5 was considered differentially abundant.

2.7. Quantitative analysis of target DNA by real-time PCR

Primers for target protein gene, reference gene Actin (Genbank: AB181991.1), Beta-tubulin 3 (Genbank: U76746.1) and Beta-tubulin 5 (GenBank: U76896.1) were designed using GenBank and synthesized by Sangon Biotech, and primer pairs were listed in Table S1. Total DNAs were isolated using total DNA extractor (Sangon Biotech, China). Real-time PCR experiments were performed by QuantStudio 5 with DNA Quantitation PCR Kit (Sangon Biotech, China) and SYBRR Premix Ex Taq™ (Takara, China), respectively. 20 μL reaction system of DNAs contained 2 μL template DNA, 0.5 μL of 10 μM forward primer and 0.5 μL of 10 μM reverse primer, 10 μL 2× DNA qPCR master mix, 6 μL ddH_2O and 1 μL ROX Reference Dye (L). 20 μL reaction system of target genes contained 2 μL template DNA, 0.4 μL of 10 μM forward primer and 0.4 μL of 10 μM reverse primer, 10 μL SYBR Premix EX Taq, 6.8 μL ddH_2O and 0.4 μL ROX Reference Dye II. The PCR reaction program was: 1) 95 °C for 30 s; 2) 40 cycles of 95 °C for 5 s and 60 °C for 30 s. Expression level of target genes was calculated with $2^{-\Delta\Delta Ct}$ methods (Simon, 2003).

2.8. Protein annotation and heatmaps

Based on the results of protein search against UniProt database (www.uniprot.org), cluster analysis of orthologous groups of protein map was employed to obtain the functional classification of the proteins and to find out the protein distribution in each functional group through the method by Dixon et al. (2007). Heatmap values were calculated by the ration of the control and the treatment, and the values were means of the four independent phenanthrene treatments and four independent controls, respectively. The heatmaps were generated using a R software package (gplots: Various R programming tools for plotting data. R package version 2.12.1; http://CRAN.Rproject.org/package=gplots2013).

2.9. Statistical analyses

The experiments were performed with four biological replicates per treatment. Statistical analyses of the data were performed using ANOVA tests by SPSS 21.0 (IBM, USA). The means were compared by the least significant difference (LSD) test at the $P < 0.05$ level.

3. Results and discussion

3.1. Chloroplast ultrastructure change

Under phenanthrene treatment, chlorosis was observed from the base of wheat leaf, and chlorophyll metabolism was destroyed (Shen et al., 2017). Through TEM observation (Fig. 1), we found that the chloroplasts became rounded and disintegrated significantly under 1.0 mg L^{-1} phenanthrene treatment (Fig. 1-7-12). In detail, for the control, the chloroplast and mitochondria were clear and distinct in the cytoplasm, the chloroplast was ellipse in shape and its inner thylakoid layer was distributed distinctly (Fig. 1-1-3). Under 0.5 mg L^{-1} phenanthrene treatment, the chloroplast was small, some organelle fragments were accumulated together and many starch grains were left in wheat leaf cells (Fig. 1-4-5). From the magnified observations (×8.0 k), the thylakoid layer tended to be loose and dissociated (Fig. 1-6). In the treatments, the chloroplasts became rounded from ellipse, chloroplast inner structure and its thylakoid layer dissolved and the amount of osmilphilic granules increased compared to the control (Fig. 1-7-12).

In terms of the above observations, the chloroplast morphology had the most significant change when wheat leaf cell was exposed to phenanthrene. The similar phenomenon occurred when *Arabidopsis thaliana* was in the chilling condition (Vella et al., 2012). But the report did not provide any mechanism on the variation. To date, there are few reports about the chloroplast morphological change when the plants are exposed to exogenous chemicals. Generally, chlorophyll contents determine leaf color (Madeira et al., 2003), and the destruction of chloroplast structure would make leaf color lighter (Wang et al., 2015a, 2015b). Hereby, it is inferred that the destroyed chloroplast is the main reason for the wheat leaf chlorosis triggered by phenanthrene exposure. Moreover, the increased osmilphilic granules under 1.0 mg L^{-1} phenanthrene and expanded starch grains under 0.5 mg L^{-1} phenanthrene were also more significant than the control (Fig. 1). Because the increase in osmilphilic granules is a symbol of oxidative stress in plant cells (Briat et al., 2007), accumulation of PAHs would lead to an oxidative response in plant leaf. The stranded starch grain is the result of

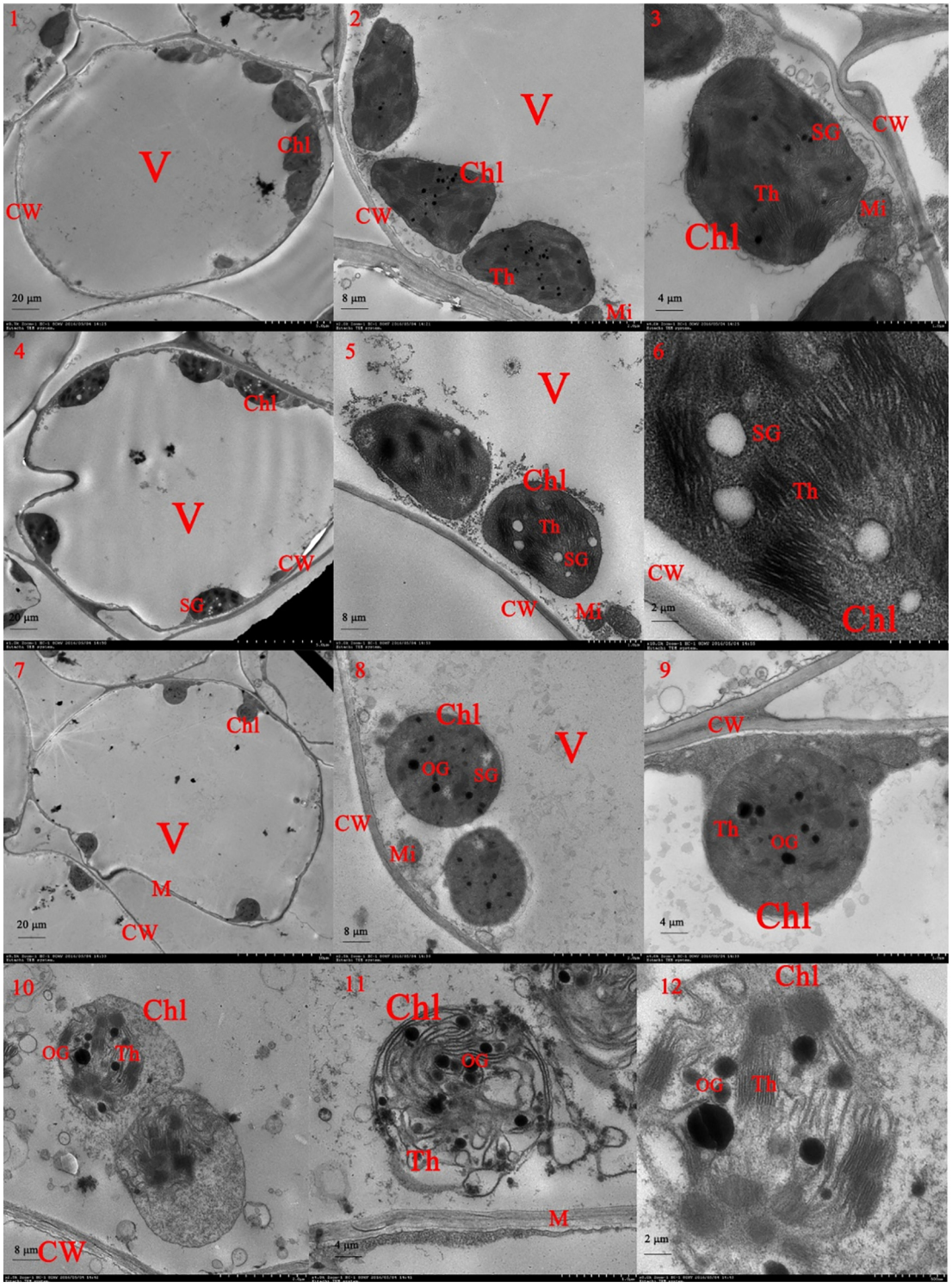

Fig. 1. Transmission electron microscope (TEM) images of wheat leaf cells under phenanthrene treatment for 9 days. Control samples: 1 (×0.5 k), 2 (×2.5 k), 3 (×4.0 k); 0.5 mg L^{-1} phenanthrene treatment: 4 (×0.5 k), 5 (×2.5 k), 6 (×8.0 k); 1.0 mg L^{-1} phenanthrene treatment: 7 (×0.5 k), 8 (×2.5 k), 9 (×4.0 k), 10 (×2.5 k), 11 (×4.0 k), 12 (×8.0 k). (Chl, chloroplast; Th, Thylakoid; CW, cell wall; IS, intercellular space; Mi, mitochondria; M, cell membrane; OG, osmilphilic granule; SG, starch grain; V, vacuole.)

blocking carbohydrate and energy metabolism (Lindell et al., 2005), due to the inhibition of some metabolic enzymes by phenanthrene.

3.2. Proteomic expression profiles

As shown in the Supporting Information (Table S2), 517 proteins were detected in our study, and the results are in line with those of Hou et al. (2009) and Jacoby et al. (2010). In Table S2, only proteins identified in all four replicates were considered. A protein with both a fold-change of > 1.5 and a *P*-value of < 0.05 was considered as differential expression. Based on the heatmaps, 261 proteins were up-regulated and 249 proteins were down-regulated under phenanthrene treatment. According to the classification map analysis (Fig. 2), these proteins were classified into four function groups, involved in biological

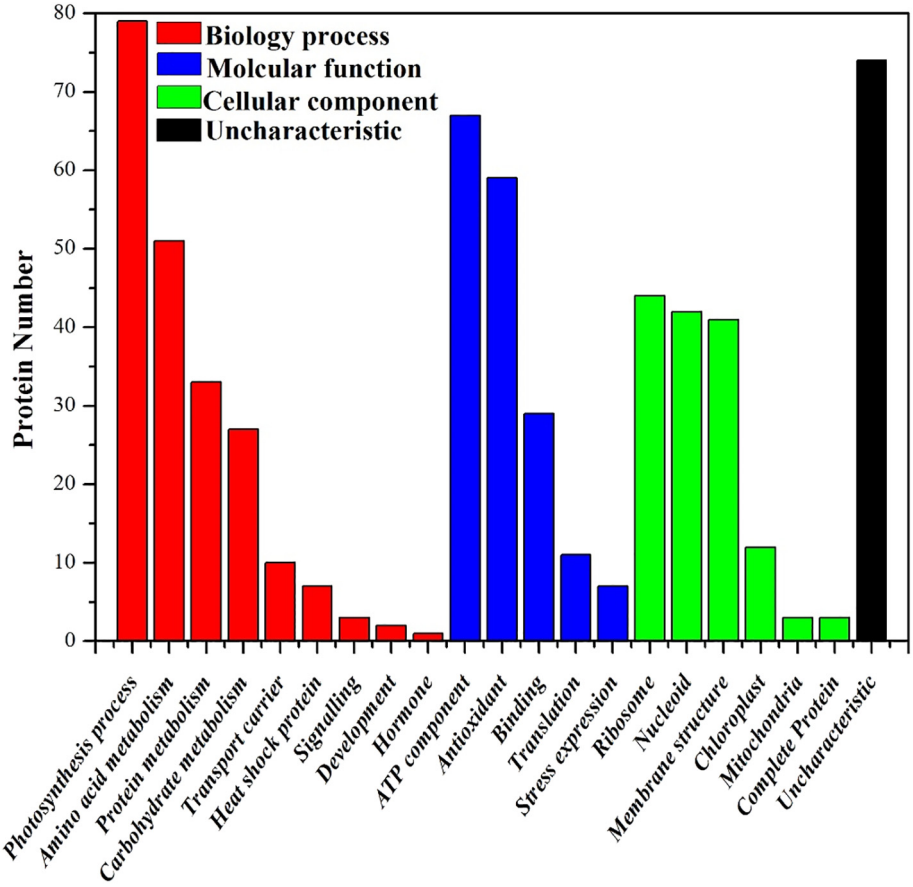

Fig. 2. Functional clusters of orthologous groups of protein (COG) classification for the differentially accumulated (expressed) proteins in wheat leaf chloroplasts of control and phenanthrene treatment.

process, molecular function, cellular component (Gene Ontology Consortium, 2001), and uncharacterized (74 proteins). Among the chloroplast proteins working in biological process, photosynthesis covered the most of the biological process, about 15.28% in the total proteins and 37.09% in the biological process. Then the numbers of amino acid and protein metabolism processes followed, containing about 23.94% and 15.49% in the biological process, respectively. Among the molecular function proteins, there were five subgroups (ATP component, antioxidant, binding, translation and stress expression) in Fig. 2. ATP and antioxidant were the main components, up to 38.73% and 34.10% in the molecular function group. In cellular function group, ribosome, nucleoid and membrane structure components were the most three subgroups, totally containing about 87.59% of proteins in this group.

Chloroplasts can carry out a number of other functions, including fatty acid and amino acid synthesis and the stress response in plants (Halliwell, 1979; Petit et al., 2005). In our results, 79 proteins worked in photosynthesis chain reaction (20 down-regulated proteins), 27 proteins in carbohydrate metabolism (14 up-regulated proteins), 73 proteins in amino acid and protein synthesis and metabolism (39 up-regulated proteins), and 63 proteins were related with stress response (35 up-regulated proteins). In addition, there were 87 proteins partaking in DNA replication and RNA transcription which accounted for 16.89% of all the proteins.

3.3. Response of chloroplast structure to phenanthrene

It has been addressed that the change of chloroplast is based on the destruction of thylakoid structure (YashRoy, 1990). In Fig. 1-9,10, the chloroplast external frame structure was still reserved under phenanthrene exposure. The evidence from proteomic analysis showed that the eight down-regulated proteins were related with thylakoid in Table S2 and Fig. 3. Thylakoid is a membrane-bound compartment inside chloroplast and the site of the light-dependent reactions of photosynthesis. It consists of a thylakoid membrane surrounding a thylakoid lumen, and grana is also frequently formed into stacks by chloroplast thylakoid (Anderson, 1986). Thylakoid is the skeleton of chloroplast, and the stabilization of thylakoid leads to the shape of chloroplast. Thylakoid is a place for PAH accumulation in *Lemna gibba*, and is considered to be a response point in plants (Duxbury et al., 1997). The accumulation of anthracene, a kind of PAHs, could increase the permeability of thylakoid membrane in *Chlamydomonas reinhardtii*, indicating that the thylakoid structure would be compromised under PAH treatment (Aksmann et al., 2011). Therefore, based on the significant change of the chloroplast morphology in Fig. 1 and the heatmaps of iTRAQ proteomic analysis (Fig. 3), we infer that the phenanthrene exposure would leads to the thylakoid protein degradation and the related protein number decrease, and then the thylakoid structure collapses. This is the major reason why chloroplast becomes rounded under phenanthrene treatment. Then we applied real-time PCR to quantitative analysis of the DNAs of target proteins. In Fig. 4, all the target genes' real-time PCR results presented were consistent with the iTRAQ results except *w5alr1* and *w5a296*, and the other 10 DNA expressions of target proteins confirmed the proteomic results. In the database (Table S2), *w5alr1* is related with thylakoid membrane structure. On the basis of the above discussion, proteomic and real-time PCR results were incompatible in *w5alr1* expression. In general, this phenomenon happens commonly in molecular experiments, because there is a hysteresis from gene transcription to protein expression and the degradation rate of mRNA is much faster than that of the protein

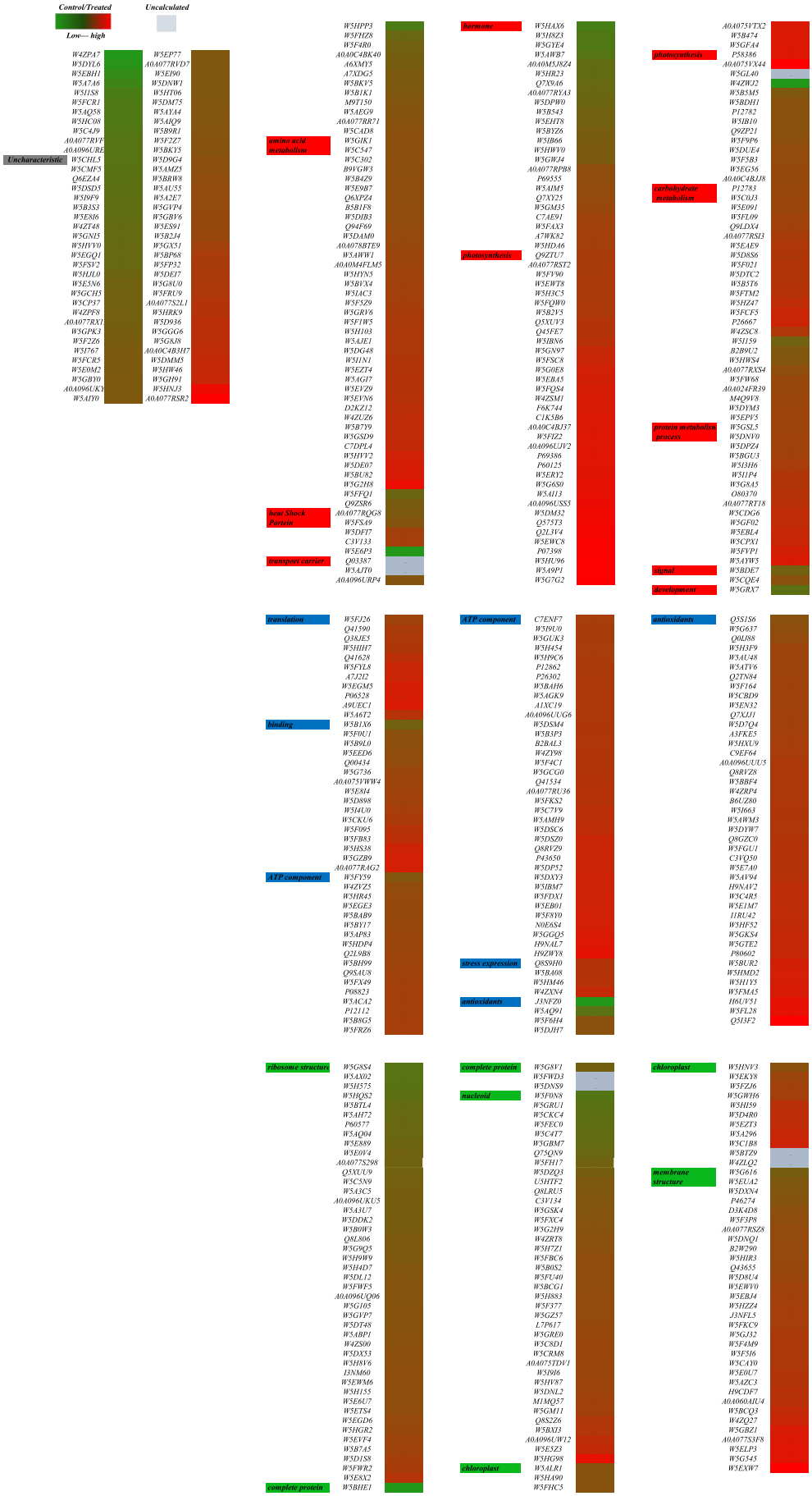

(caption on next page)

Fig. 3. Heatmap overview of iTRAQ data. Columns denote the metric; rows correspond to raw values. The color gradient (Control/Treated) for each cell ranges from low (green) to underperforming (black), and, finally, high (red). The grey means the uncalculated proteins. (For interpretation of the references to color in this figure legend, the reader is referred to the web version of this article.)

under stress condition (Heidarvand and Amiri, 2010; Schwanhausser et al., 2011). In addition, *w5alr1* expression was also suppressed together with the other 6 genes related with thylakoid structure, and the proteins relative to thylakoid became down-regulated under phenanthrene treatment. Therefore, the structural breakage of thylakoid is the major reason for chloroplast abnormality under phenanthrene treatment. The chloroplast protein verification experiment was carried out by sodium dodecyl sulphate polyacrylamide gel electrophoresis (SDS-PAGE), and the results matched well with the iTRAQ results. The detailed information was listed in the Supporting Information (Fig. S1).

Meanwhile, there were another 4 chloroplast proteins responded under phenanthrene treatment, which were W5HA90, W5FHC5, W5HNV3 and W5FZJ6 related with stroma and envelope of chloroplast. In cells, stroma is the connective, functionally supportive framework (Forsberg et al., 1993), and it is the frame structure in chloroplast; envelope is a double-membrane structure and the outer protector of chloroplast (Block et al., 1983). In Fig. 1-11-12, it was clearly observed that the chloroplast was still reserved in leaf cell, but its morphology changed with the thylakoid structure becoming loose and dissociated. Combined with the results of iTRAQ and real-time PCR, the proteins related to stroma, W5FHC5 and W5HNV3, were up-regulated under phenanthrene treatment and the corresponding gene expression also exhibited the same trend, while W5FZJ6 stroma protein displayed an opposite to the two proteins (W5FHC5 and W5HNV3). The expression of *w5fzj6* is the potential reason for chloroplast disintegration in the later stage (Fig. 1-10-12). Meanwhile, the two chloroplast envelope proteins turned up-regulated in iTRAQ (Fig. 3) and negative in real-time PCR results (Fig. 4), suggesting that chloroplast membrane structure would become unstable under phenanthrene treatment. The active expression of W5HA90 and W5FHC5 is the important reason for the chloroplast structure stabilization under PAH exposure.

Compared to the recent reports about PAH-triggered carcinogenic and teratogenic effects in animals and humans, there are some commons about cell structure between plants and animals. It was found that the lung cell structure would be destroyed when the mice were exposed to smoke or air pollution of PAHs, and its verification experiment showed that the normal human lung epithelial 16HBE cells would also be destroyed in structure under the treatments of PAH-polluted smoke (Wang et al., 2015a, 2015b). Furthermore, comparing the homologous cells, chloroplast and red blood cell (Hughes and Latner, 1936), there still comes many similarities when exposed to PAHs. Under PAH pollution, the absorbed PAHs would induce hemolytic anemia (a form of anemia) due to hemolysis which can lead to the abnormal breakdown of red blood cells (Sanctucci and Shah, 2000; Gehrs and Friedberg, 2002). In recent research, it has been found that the entered PAHs cause rapid cell damage (e.g., bone marrow cells), and it is largely attributed to their reactive oxygenated metabolites, potential of oxidative stress, and the adducts of their metabolites with DNA in clinical trials (Kamal et al., 2015; Chibwe et al., 2015). It is the major reason for carcinogenicity, teratogenicity and mutagenicity in animals and humans (Yan et al., 2004; Kim et al., 2013). Meanwhile, the structure of human macrophage, which has similar origin with chloroplast, would totally turn small and free from oval biconcave disk under benzo(a)pyrene treatment, together with cell viability decrease and apoptotic process increase (van Grevenynghe et al., 2003). The same phenomena would also happen for adult pearl oyster in the PAH-contaminated water, and its branchial lamellae cells would turn necrosis and edemas (Al-Hashem, 2017). Therefore, cell structure destructions are consistent when organisms are exposed to PAHs. However, the PAH-toxicity mechanism is still unclear in plant cells. Here in our result, the abnormality of chloroplast morphology and structure is the first evidence and the reason for the PAH-triggered mutagenic phenomenon in plant cells. As the deformation of chloroplast is a kind of carcinogenic and teratogenic effects, we suggest that our observation is the PAH-triggered carcinogenic and teratogenic effect in plants. Briefly, at the molecular level, the phenanthrene exposure would be a stress signal that inhibits the thylakoid protein gene expression, and the lack of thylakoid proteins is the main reason for chloroplast structural deformation and the

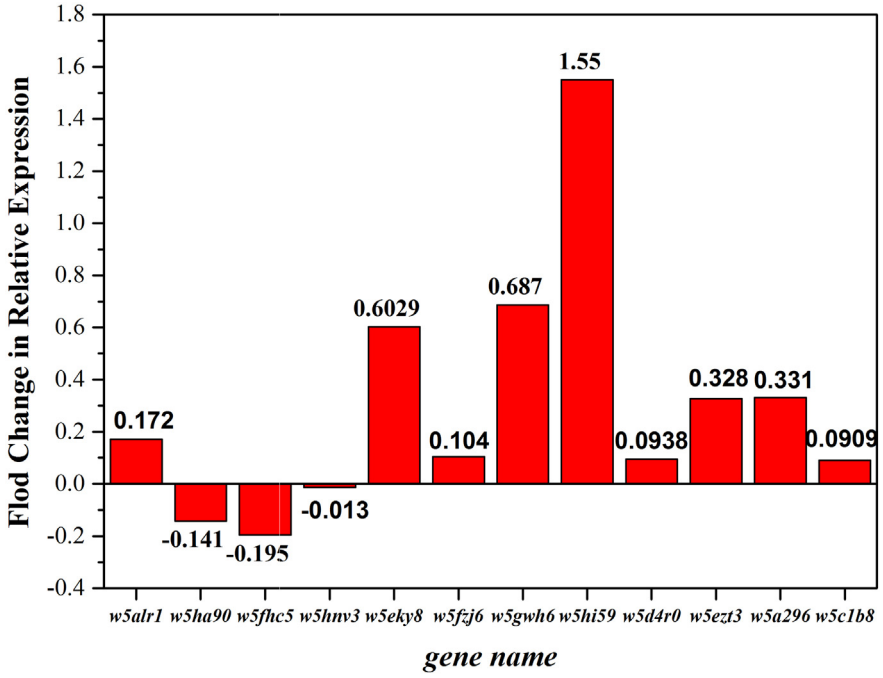

Fig. 4. Real-time PCR identification of target protein genes of wheat leaf chloroplast under phenanthrene treatment.

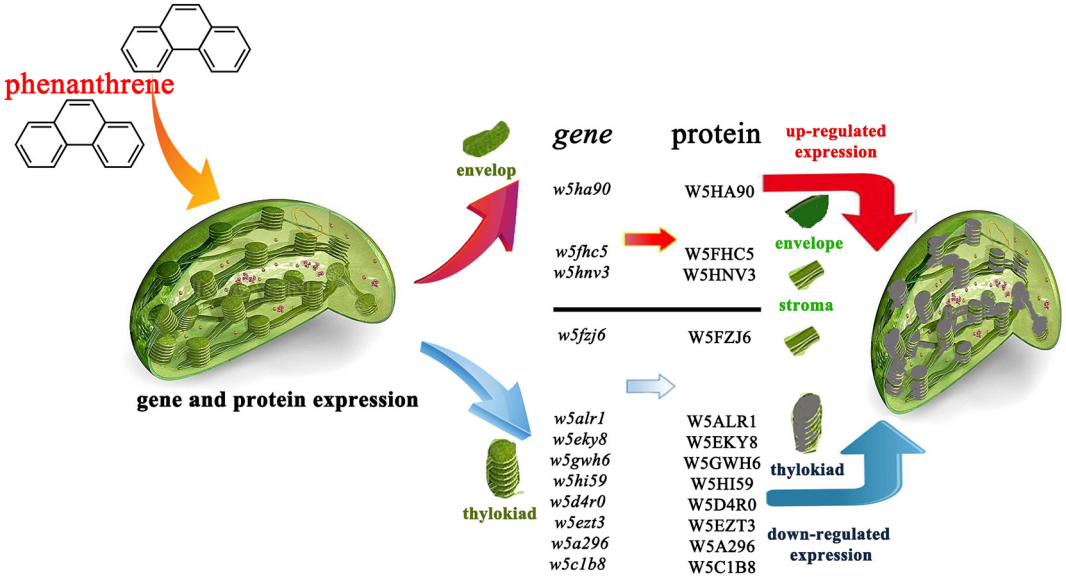

Fig. 5. Proposed mechanism for gene and protein response to chloroplast deformation exposed to phenanthrene. The red and blue arrows indicate up-regulation and down-regulation, respectively; the grey part of the chloroplast means the down-regulation of proteins. (For interpretation of the references to color in this figure legend, the reader is referred to the web version of this article.)

chlorosis in wheat leaf cells. Thus, we describe the chloroplast deformation mechanism in Fig. 5. Through the inhibition of thylakoid gene expression of wheat leaf cell exposed to phenanthrene, the related proteins become down-regulated in chloroplast, and the weakness of thylakoid leads to the chloroplast deformation under phenanthrene treatments. And the chloroplast deformation is similar to the red blood cell change under PAH treatments (Sanctucci and Shah, 2000; Gehrs and Friedberg, 2002).

4. Conclusions

In summary, this study is the first quantitative analysis in plant chloroplast protein change under phenanthrene treatment by iTRAQ proteomics. We conclude that the destruction of thylakoid structural proteins is the reason for chloroplast deformation under phenanthrene treatment. To date, this is the first report about the carcinogenic and teratogenic effect in plant cells exposed to PAHs. Our results offer important information on the toxicity in plant cells exposed to PAHs.

Associated content

Protein information through iTRAQ.

Author contributions

X. Z. and B. X. planned and designed the research; Y. S., J. L. and R. G. contributed to perform experiments and analyzed data. Y. S. and X. Z. wrote the manuscript, with contribution and revision by all other authors.

Acknowledgements

This work was supported jointly by the National Natural Science Foundation of China (31770546, 31370521), the Priority Academic Program Development of Jiangsu Higher Education Institutions (PAPD) and the Graduate Student Training Innovation Project of Jiangsu Province (KYZZ16_0378). Yu Shen thanks the China Scholarship Council (CSC) for the financial support to study at the University of Massachusetts, Amherst.

Conflict of interest

The authors have no conflict of interest to declare.

Appendix A. Supplementary data

Supplementary data to this article can be found online at https://doi.org/10.1016/j.envint.2018.11.074.

References

Aebersold, R., Mann, M., 2016. Mass-spectrometric exploration of proteome structure and function. Nature 537, 347–355. https://doi.org/10.1038/nature19949.
Agrafiotis, D.K., Lobanov, V.S., Salemme, F.R., 2002. Combinatorial informatics in the post-genomics ERA. Nat. Rev. Drug Discov. 1, 337–346. https://doi.org/10.1038/nrd791.
Aksmann, A., Shutova, T., Samuelsson, G., Tukaj, Z., 2011. The mechanism of anthracene interaction with photosynthetic apparatus: a study using intact cells, thylakoid membranes and PS II complexes isolated from Chlamydomonas reinhardtii. Aquat. Toxicol. 104, 205–210. https://doi.org/10.1016/j.aquatox.2011.04.017.
Al-Hashem, M., 2017. Gill histopathological effects of PAHs on adult pearl oyster, Pinctada radiata at Al-Khiran coast in Kuwait. J. Environ. Prot. 8 (2), 109–119. https://doi.org/10.4236/jep.2017.82009.
Ali, N., Ismail, I.M.I., Khoder, M., Shamy, M., Alghamdi, M., Al Khalaf, A., Costa, M., 2017. Polycyclic aromatic hydrocarbons (PAHs) in the settled dust of automobile workshops, health and carcinogenic risk evaluation. Sci. Total Environ. 601-602, 478–484. https://doi.org/10.1016/j.scitotenv.2017.05.110.
Anderson, M.J., 1986. Photoregulation of the composition, function, and structure of thylakoid membranes. Annu. Rev. Plant Biol. 37, 93–136. https://doi.org/10.1146/annurev.pp.37.060186.000521.
Anderson, N.L., Anderson, N.G., 1998. Proteome and proteomics: new technologies, new concepts and new words. Electrophoresis 19, 1853–1861. https://doi.org/10.1002/elps.1150191103.
Anderson, J.D., Johansson, H.J., Graham, C.S., Vesterlund, M., Pham, M.T., Bramlett, C.S., Montgomery, E.N., Mellema, M.S., Bardini, R.L., Contreras, Z., Hoon, M., Bauer, G., Fink, K.D., Fury, B., Hendrix, K.J., Chedin, F., El-Andaloussi, S., Hwang, B., Mulligan, M.S., Lehtio, J., Nolta, J.A., 2016. Comprehensive proteomic analysis of mesenchymal stem cell exosomes reveals modulation of angiogenesis via nuclear factor-KappaB signaling. Stem Cells 34, 601–613. https://doi.org/10.1002/stem.2298.
Andersson, B., Anderson, J.M., 1980. Lateral heterogeneity in the distribution of chlorophyll-protein complexes of the thylakoid membranes of spinach chloroplasts. BBA-Bioenergetics 593, 427–440. https://doi.org/10.1016/0005-2728(80)90078-X.
Bensmail, H., Haoudi, A., 2003. Ostgenomics: proteomics and bioinformatics in cancer research. J Biomed Biotechnol (4), 217–230. https://doi.org/10.1155/S1110724303209207.
Block, M.A., Dorne, A.J., Joyard, J., Douce, R., 1983. Preparation and characterization of membrane fractions enriched in outer and inner envelope membranes from spinach chloroplas. J. Biol. Chem. 258, 13281–13285.
Bordajandi, L.R., Gomez, G., Abad, E., Rivera, J., Ndez-Baston, M.M.F., Blasco, J., Gonzalez, M., 2004. Survey of persistent organochlorine contaminants (PCBs, PCDD/

Fs, and PAHs), heavy metals (Cu, Cd, Zn, Pb, and Hg), and arsenic in food samples from Huelva (Spain): levels and health implications. J. Agric. Food Chem. 52, 992–1001. https://doi.org/10.1021/jf030453y.
Bozzola, J.J., 2007. Conventional specimen preparation techniques for transmission electron microscopy of cultured cells. Methods Mol. Biol. 369, 1–18. https://doi.org/10.1007/978-1-59745-294-6_1.
Briat, J.F., Curie, C., Gaymard, F., 2007. Iron utilization and metabolism in plants. Curr. Opin. Plant Biol. 10, 276–282. https://doi.org/10.1016/j.pbi.2007.04.003.
Carvalho, R.N., Lettieri, T., 2011. Proteomic analysis of the marine diatom Thalassiosira pseudonana upon exposure to benzo(a)pyrene. BMC Genomics 12, 159. https://doi.org/10.1186/1471-2164-12-159.
Chibwe, L., Geier, M.C., Nakamura, J., Tanguay, R.L., Aitken, M.D., Simonich, S.L.M., 2015. Aerobic bioremediation of PAH contaminated soil results in increased genotoxicity and developmental toxicity. Environ. Sci. Technol. 49 (23), 13889–13898. https://doi.org/10.1021/acs.est.5b00499.
Davie-Martin, C.L., Stratton, K.G., Teeguarden, J.G., Waters, K.M., Simonich, S.L.M., 2017. Implications of bioremediation of polycyclic aromatic hydrocarbon-contaminated soils for human health and cancer risk. Environ. Sci. Technol. 51 (17), 9458–9468. https://doi.org/10.1021/acs.est.7b02956.
de Lucia, E.H., Gomez-Casanovas, N., Greenberg, J.A., Hudiburg, T.W., Kantola, I.B., Long, S.P., Miller, A.D., Ort, D.R., Parton, W.J., 2014. The theoretical limit to plant productivity. Environ. Sci. Technol. 48 (16), 9471–9477. https://doi.org/10.1021/es502348e.
Dixon, A.L., Liang, L., Moffatt, M.F., Chen, W., Heath, S., Wong, K.C., Taylor, J., Burnett, E., Gut, I., Farrall, M., Lathrop, G.M., Abecasis, G.R., Cookson, W.O., 2007. A genome-wide association study of global gene expression. Nat. Genet. 39, 1202–1207. https://doi.org/10.1038/ng2109.
Duxbury, C.L., Dixon, D.G., Greenberg, B.M., 1997. Effects of simulated solar radiation on the bioaccumulation of polycyclic aromatic hydrocarbons by the duckweed *Lemna gibba*. Environ. Toxicol. Chem. 16, 1739–1748. https://doi.org/10.1002/etc.5620160824.
El Amrani, A., Dumas, A.S., Wick, L.Y., Yergeau, E., Berthome, R., 2015. "Omics" insights into PAH degradation toward improved green remediation biotechnologies. Environ. Sci. Technol. 49 (19), 11281–11291. https://doi.org/10.1021/acs.est.5b01740.
Forsberg, K., Nagy, I.V., Heldin, C.H., Herlynt, M., Westermark, B., 1993. Platelet-derived growth factor (PDGF) in oncogenesis: development of a vascular connective tissue stroma in xenotransplanted human melanoma producing PDGF-BB. Proc. Natl. Acad. Sci. U. S. A. 90, 393–397. https://doi.org/10.1073/pnas.90.2.393.
Gehrs, B.C., Friedberg, R.C., 2002. Autoimmune hemolytic anemia. Am. J. Hematol. 69, 258–271. https://doi.org/10.1002/ajh.10062.
Gene Ontology Consortium, 2001. Creating the gene ontology resource: design and implementation. Genome Res. 11 (8), 1425–1433. https://doi.org/10.1101/gr.180801.
Gonczarowska-Jorge, H., Zahedi, R.P., Sickmann, A., 2017. The proteome of baker's yeast mitochondria. Mitochondrion 33, 15–21. https://doi.org/10.1016/j.mito.2016.08.007.
Grabsztunowicz, M., Jackowski, G., 2012. Isolation of intact and pure chloroplasts from leaves of *Arabidopsis* thaliana plants acclimated to low irradiance for studies on Rubisco regulation. Acta Soc. Bot. Pol. 81, 91–95. https://doi.org/10.5586/asbp.2012.043.
Halliwell, B., 1979. The chloroplast at work a review of modern developments in our understanding of chloroplast metabolism. Prog. Biophys. Mol. Biol. 33, 1–54. https://doi.org/10.1016/0079-6107(79)90024-5.
Heidarvand, L., Amiri, R.M., 2010. What happens in plant molecular responses to cold stress? Acta Physiol. Plant. 32, 19–431. https://doi.org/10.1007/s11738-009-0451-8.
Hood, L., Rowen, L., 2013. The human genome project: big science transforms biology and medicine. Genome Med. 5, 79. https://doi.org/10.1186/gm483.
Hou, D., Xu, H., Du, G., Lin, J., Duan, M., Guo, A., 2009. Proteome analysis of chloroplast proteins in stage albinism line of winter wheat (*Triticum aestivum*) FA85. BMB Rep. 42, 450–455.
Hughes, J.H., Latner, A.L., 1936. Chlorophyll and haemoglobin regeneration after haemorrhage. J. Physiol. 1936 (86), 188–395. https://doi.org/10.1113/jphysiol.1936.sp003374.
Jacoby, R.P., Millar, A.H., Taylor, N.L., 2010. Wheat mitochondrial proteomes provide new links between antioxidant defense and plant salinity tolerance. J. Proteome Res. 9, 6595–6604. https://doi.org/10.1021/pr1007834.
Jia, H., Zhao, S., Nulaji, G., Tao, K.L., Wang, F., Sharma, V.K., Wang, C., 2017. Environmentally persistent free radicals in soils of past coking sites: distribution and stabilization. Environ. Sci. Technol. 51 (11), 6000–6008. https://doi.org/10.1021/acs.est.7b00599.
Kamal, A., Cincinelli, A., Martellini, T., Malik, R.N., 2015. A review of PAH exposure from the combustion of biomass fuel and their less surveyed effect on the blood parameters. Environ. Sci. Pollut. Res. 22, 4076–4098. https://doi.org/10.1007/s11356-014-3748-0.
Käpylä, M., Heikkinen, J.P., Asunta, T., 2009. Influence of content knowledge on pedagogical content knowledge: the case of teaching photosynthesis and plant growth. Int. J. Sci. Educ. 31, 1395–1415. https://doi.org/10.1080/09500690802082168.
Kim, K.H., Jahan, S.A., Kabir, E., Brown, R.J., 2013. A review of airborne polycyclic aromatic hydrocarbons (PAHs) and their human health effects. Environ. Int. 60, 71–80. https://doi.org/10.1016/j.envint.2013.07.019.
Lan, P., Li, W., Wen, T., Shiau, J., Wu, Y., Lin, W., Schmidt, W., 2010. iTRAQ protein profile analysis of *Arabidopsis* roots reveals new aspects critical for Fe homeostasis. Plant Physiol. 110, 169508. https://doi.org/10.1104/pp.110.169508.
Lande, N.V., Subba, P., Barua, P., Gayen, D., Prasad, T.K., Chakraborty, S., Chakraborty, N., 2017. Dissecting the chloroplast proteome of chickpea (*Cicer arietinum* L.) provides new insights into classical and non-classical functions. J. Proteome 165, 11–20. https://doi.org/10.1016/j.jprot.2017.06.005.
Li, J., Gao, Y., Wu, S., Cheung, K., Wang, X., Wong, M., 2008. Physiological and biochemical responses of rice (*Oryza Sativa* L.) to phenanthrene and pyrene. Int. J. Phytoremediation 10, 106–118. https://doi.org/10.1080/15226510801913587.
Lindell, D., Jaffe, J.D., Johnson, Z.I., Church, G.M., Chisholm, S.W., 2005. Photosynthesis genes in marine viruses yield proteins during host infection. Nature 438, 86–89. https://doi.org/10.1038/nature04111.
Madeira, A.C., Ferreira, A., Varennes, A.D., Vieira, M.I., 2003. SPAD meter versus tristimulus colorimeter to estimate chlorophyll content and leaf color in sweet pepper. Commun. Soil Sci. Plant Anal. 34, 2461–2470. https://doi.org/10.1081/CSS-120024779.
Mirzaei, M., Pascovici, D., Atwell, B.J., Haynes, P.A., 2012. Differential regulation of aquaporins, small GTPases and V-ATPases proteins in rice leaves subjected to drought stress and recovery. Proteomics 12 (6), 864–877. https://doi.org/10.1002/pmic.201100389.
Mustafa, G., Komatsu, S., 2016. Toxicity of heavy metals and metal-containing nanoparticles on plants. BBA-Bioenergetics 1864 (8), 932–944. https://doi.org/10.1016/j.bbapap.2016.02.020.
Muth, T., Keller, D., Puetz, S.M., Martens, L., Sickmann, A., Boehm, A.M., 2010. jTraqX: a free, platform independent tool for isobaric tag quantitation at the protein level. Proteomics 10, 1223–1225.
Petit, R.J., Duminil, J., Fineschi, S., Hampe, A., Salvini, D., Vendramin, G.G., 2005. Comparative organization of chloroplast, mitochondrial and nuclear diversity in plant populations. Mol. Ecol. 14, 689–701. https://doi.org/10.1111/j.1365-294X.2004.02410.x.
Ron, D., Walter, P., 2007. Signal integration in the endoplasmic reticulum unfolded protein response. Nat. Rev. Mol. Cell Biol. 8, 519. https://doi.org/10.1038/nrm2199.
Sanctucci, K., Shah, B., 2000. Association of naphthalene with acute hemolytic anemia. Acad. Emerg. Med. 7, 42–47. https://doi.org/10.1111/j.1553-2712.2000.tb01889.x.
Schwanhausser, B., Busse, D., Li, N., Dittmar, G., Schuchhardt, J., Wolf, J., Chen, W., Selbach, M., 2011. Global quantification of mammalian gene expression control. Nature 473, 337–342. https://doi.org/10.1038/nature10098.
Sharkey, T.D., 2005. Effects of moderate heat stress on photosynthesis: importance of thylakoid reactions, rubisco deactivation, reactive oxygen species, and thermotolerance providedby isoprene. Plant Cell Environ. 28, 269–277. https://doi.org/10.1111/j.1365-3040.2005.01324.x.
Shen, Y., Du, J., Yue, L., Zhan, X., 2016. Proteomic analysis of plasma membrane proteins in wheat roots exposed to phenanthrene. Environ. Sci. Pollut. Res. 23, 10863–10871. https://doi.org/10.1007/s11356-016-6307-z.
Shen, Y., Li, J., Gu, R., Yue, L., Zhan, X., Xing, B., 2017. Phenanthrene-triggered chlorosis is caused by elevated chlorophyll degradation and leaf moisture. Environ. Pollut. 220, 1311–1321. https://doi.org/10.1016/j.envpol.2016.11.003.
Simon, P., 2003. Q-Gene: processing quantitative real-time RT-PCR data. Bioinformatics 19, 1439–1440. https://doi.org/10.1093/bioinformatics/btg157.
Tervahauta, A.I., Fortelius, C., Tuomainen, M., Akerman, M.L., Rantalainen, K., Sipila, T., Lehesranta, S.J., Koistinen, K.M., Karenlampi, S., Yrjala, K., 2009. Effect of birch (*Betula* spp.) and associated rhizoidal bacteria on the degradation of soil polyaromatic hydrocarbons, PAH-induced changes in birch proteome and bacterial community. Environ. Pollut. 157, 341–346. https://doi.org/10.1016/j.envpol.2008.06.031.
van Grevenynghe, J., Rion, S., Le Ferrec, E., Le Vee, M., Amiot, K., Fauchet, R., Fardel, O., 2003. Polycyclic aromatic hydrocarbons inhibit differentiation of human monocytes into macrophages. J. Immunol. 170 (5), 2374–2381. https://doi.org/10.4049/jimmunol.170.5.2374.
Vélez-Bermúdez, I.C., Wen, T.N., Lan, P., et al., 2016. Isobaric tag for relative and absolute quantitation (iTRAQ)-based protein profiling in plants//Plant Proteostasis. Humana Press, New York, NY, pp. 213–221.
Vella, N.G., Joss, T.V., Roberts, T.H., 2012. Chilling-induced ultrastructural changes to mesophyll cells of *Arabidopsis* grown under short days are almost completely reversible by plant re-warming. Protoplasma 249, 1137–1149. https://doi.org/10.1007/s00709-011-0363-5.
Wang, G., Chen, X., Zhou, B., Wen, Z., Huang, Y., Chen, H., Li, G., Huang, Z., Zhou, Y., Feng, L., Wei, M., Qu, L., Zhou, G., 2015a. The chemokine CXCL13 in lung cancers associated with environmental polycyclic aromatic hydrocarbons pollution. elife 4, e09419. https://doi.org/10.7554/eLife.09419.
Wang, Z., Fan, S., Chen, L., Zhao, Y., Yang, Y., Ai, J., Li, X., Liu, Y., Qin, H., 2015b. *Actinidia kolomikta* leaf colour and optical characteristics. Biol. Plant. 59, 767–772. https://doi.org/10.1007/s10535-015-0544-8.
Wei, H., Song, S., Tian, H., Liu, T., 2008. Effects of phenanthrene on seed germination and some physiological activities of wheat seedling. C. R. Biol. 337, 95–100. https://doi.org/10.1016/j.crvi.2013.11.005.
Wiśniewski, J.R., Zougman, A., Nagaraj, N., Mann, M., 2009. Universal sample preparation method for proteome analysis. Nat. Methods 6 (5), 359. https://doi.org/10.1038/nmeth.1322.
Yan, J., Wang, L., Fu, P.P., Yu, H., 2004. Photomutagenicity of 16 polycyclic aromatic hydrocarbons from the US EPA priority pollutant list. Mutat. Res. 557, 99–108. https://doi.org/10.1016/j.mrgentox.2003.10.004.
YashRoy, R.C., 1990. Magnetic resonance studies of dynamic organization of lipids in chloroplast membranes. J. Biosci. 15 (4), 281–288 (doi = 10.1.1.584.2585).
Yokthongwattana, C., Mahong, B., Roytrakul, S., Phaonaklop, N., Narangajavana, J., Yokthongwattana, K., 2012. Proteomic analysis of salinity-stressed *Chlamydomonas reinhardtii* revealed differential suppression and induction of a large number. Planta 235, 649–659. https://doi.org/10.1007/s00425-012-1594-1.
Zelinkova, Z., Wenzl, T., 2015. The occurrence of 16 EPA PAHs in food–a review. Polycycl. Aromat. Compd. 35, 248–284. https://doi.org/10.1080/10406638.2014.918550.